Pergamon

Cement and Concrete Research 32 (2002) 303–311

CEMENT AND CONCRETE RESEARCH

Effects of the incorporation of Municipal Solid Waste Incineration fly ash in cement pastes and mortars I. Experimental study

S. Rémond[a,b,*], P. Pimienta[a], D.P. Bentz[c]

[a]CSTB, 84 avenue Jean Jaurès, Champs sur Marne, Marne la Vallée Cedex 2, 77421, France
[b]LMT ENS de Cachan, 61 avenue du Président Wilson, Cachan Cedex 94235, France
[c]BFRL NIST, 100 Bureau Drive Stop 8621, Gaithersburg, MD 20899-8621, USA

Received 20 October 2000; accepted 27 August 2001

Abstract

This work falls within the scope of a general problem regarding the assessment of concrete manufactured from waste materials. The main objective is to study the long-term evolution of these materials during the leaching process, using the cellular automaton-based hydration model developed at the National Institute of Standards and Technology. The work is based on the analysis of mortars and cement pastes containing experimental waste: Municipal Solid Waste Incineration fly ash (MSWI fly ash). The study therefore aims to develop a methodology for assessing concrete manufactured from waste, and not to study a process or a formulation enabling the incorporation of the waste in concrete. The physical, chemical and mineralogical characteristics of MSWI fly ash were first analysed to introduce them into the model. A simplified quantitative mineralogical composition of the ash was proposed. The performance characteristics (setting times, compressive strengths, shrinkage, etc.) for mortars containing ash were then studied.

Keywords: Fly ash; Characterization; Hydration products; Waste management

1. Introduction

The incorporation of waste in concrete manufacture may provide a satisfactory solution to the problems posed by waste management. The building sector uses large quantities of natural materials; hence, its capacity to recycle and upgrade waste is considerable. Certain industrial byproducts have been used for a number of years as cement or concrete components (fly ash, silica fume, etc.). Other waste products may also be recycled and upgraded in concretes. However, the new material thus formed must be usable as a building material and, in particular, have the necessary performance characteristics (workability, mechanical strength, etc.) to satisfy the specifications determined by its applications. In addition, it should be inoffensive with regards to health and the environment. Finally, the incorporation of the waste should not impair concrete durability. Traditional assessment methods must therefore be adapted to evaluate these new materials.

This study contributes to the development of a methodology for assessing concrete manufactured from waste. The methodology is based on the study of mortar containing experimental waste: Municipal Solid Waste Incineration fly ash (MSWI fly ash) [1,2]. The ash is considered as experimental waste because of, in particular, its high content of soluble salts and heavy metals. We stress the fact that the present research work does not aim to study a process or a formulation enabling the incorporation of this waste in concrete.

The durability and the environmental impact of concrete are closely connected to its transport properties, which control the kinetics of the penetration of water and aggressive agents into concrete. The movement of chemical species within the material and the leaching of certain chemicals are also closely linked to concrete diffusivity.

* Corresponding author. IUP, GCI, 5 Mail Gay-Lussac, Neuville sur Oise, Cergy-Pontoise, Cedex 95031, France. Tel.: +33-1-34-25-69-15.
E-mail address: sebastian.remond@iupqc.u-cergy.fr (S. Rémond).

0008-8846/02/$ – see front matter
PII: S0008-8846(01)00674-3

However, the transport properties of concrete are likely to evolve considerably as the material ages (carbonation, leaching, etc.). The study of the development of the microstructure of concrete-containing waste is therefore very important in predicting the long-term behavior of these materials.

To study the long-term development of the microstructure of concrete-containing waste during the leaching process, we applied the CEMHYD3D hydration model [3], originally developed by Bentz and Garboczi [4], to cement pastes containing MSWI fly ash. In this article, we present the experimental research carried out to determine the model's input data. The second part of the study, to be published in a future article, will present the results of the model.

The physical, chemical and mineralogical characteristics of the MSWI fly ash were first analysed to incorporate it into the hydration model. Hydrates formed in pure cement pastes and pastes containing ash were then analysed to include the ash/cement interactions in the model. Finally, the performance characteristics of mortars containing increasing levels of MSWI fly ash were studied to identify the short- and middle-term influence of the ash on mortars' properties.

2. Materials

The MSWI fly ash came from the Municipal Solid Waste Incineration Plant in Lagny (France), which operates with a wet scrubber. Approximately 300 kg of ash were taken as samples over a 4-day period of normal operation in the factory during the month of June 1996 and stocked separately in closely sealed barrels. Before tests, an identical mass was taken from each sample, the ash was sieved to 630 μm and carefully homogenized. The aim of the sieving was to eliminate the larger light particles. The residue of larger light particles after the sieving process was approximately 5% of the mass of the MSWI fly ash.

Two types of cement were used. The first, Class C1, is a cement with a low C_3A (4.2%) content (CPA-CEM I 52.5 PMES HTS from the Lafarge factory at Le Teil, France).[1] The second, Class C2, is a cement with a high C_3A (11.6%) content (CPA-CEM I 52.5 from the Lafarge factory at Cormeilles, France).

The sand used in the manufacture of the mortars is a reference sand that is compliant with the NF EN 196-1 standard [5].

[1] Certain materials are identified in this paper to specify the experimental procedure. In no case does such identification imply endorsement by the National Institute of Standards and Technology, nor does it indicate that the products are necessarily the best available for the purpose.

3. Experimental procedures

3.1. Tests on MSWI fly ash: physico-chemical and mineralogical characterization

The granulometry of the MSWI fly ash was determined using laser granulometry. The oxide contents were determined using X-ray fluorescence spectrometry. The chloride content was measured by precipitation as silver chloride and using a potentiometric method. The sulfate content was obtained gravimetrically by precipitation as barium sulfate. The heavy metal content was determined by dissolution in hydrofluoric and perchloric acids followed by atomic emission spectrometry. All these tests were carried out at the Louis Vicat Technical Centre in L'Isle d'Abeau (France). The principal crystalline compounds in the ash were analyzed by X-ray powder diffraction (XRD) with copper Kα radiation ($\lambda = 1.5406$ Å). These tests were carried out at the Henry Longchambon Diffractometry Centre in Lyon (France).

Observations by scanning electron microscopy (SEM) were made on polished sections prepared by mixing ash with a low-viscosity epoxy resin [6]. Backscattered electron and X-ray images were collected for two different fields of observation, designated FA1 and FA2, respectively. The following elements were analysed: Ca, Al, Si, Fe, Cl, S, Na and K.

3.2. Tests on cement pastes

3.2.1. Identification of the hydrates formed in cement paste in the presence of MSWI fly ash

To identify hydrates formed in cement paste in the presence of MSWI fly ash, XRD analyses were carried out.

Cement pastes with a water/cement (W/C) ratio of 0.5 and ash/cement ratios of 0 and 0.2 were prepared for the XRD analyses. The pastes were placed in two layers in $7 \times 7 \times 40$ cm molds (60 impacts per layer) on the impact test bench. After placement, the molds were then kept in sealed bags. The cement pastes were removed from the molds after 2 days, placed in sealed bags and kept at a temperature of 20 °C. After curing for at least 28 days in the sealed bags, the central region of the samples was cut out (approximately 1 cm was removed from each surface of the test pieces). XRD was then carried out with the copper Kα radiation ($\lambda = 1.5406$ Å). Table 1 shows the composition of the pastes.

Table 1
Composition of the cement pastes used for the XRD tests

Designation	Cement (g)	Water (g)	MSWI fly ash (g)
P0–C1	1000	500	0
P20–C1	1000	500	200
P0–C2	1000	500	0
P20–C2	1000	500	200

3.2.2. Study of the porous structure of the C–S–H formed in the presence of MSWI fly ash

To study the porous structure of the C–S–H formed in cement pastes in the presence of MSWI fly ash, differential scanning calorimetry (DSC) tests were carried out on different cement pastes. Two cement pastes were made: a pure paste designated P–C1 (W/C = 0.4) and a paste containing MSWI fly ash designated P–FA (W/C = 0.4 and 20% MSWI fly ash in place of cement). The components were blended manually in plastic bags then cured in sealed PVC bottles.

The DSC tests were carried out after (1, 3, 8, 14, 28 and 60) days of hydration. These tests involved measuring the heat flux released by a sample subjected to temperature variation. The heat flow peaks enabled us to identify the temperatures at which changes in state took place within the material. In our tests, the cement pastes underwent a fall in temperature from +5 °C to −60 °C at a rate of −0.5 °C/min. The heat flow peaks allowed us to identify the temperatures at which water solidification takes place within the material. These temperatures are influenced essentially by two parameters: the size of the material's pores and the concentration of the interstitial solution. To differentiate between the influence of these two parameters, the interstitial solutions of the two cement pastes P–C1 and P–FA were replaced by distilled water. The two cement pastes were immersed successively in ethanol for 3 days, in ethylene glycol for 3 days and finally in distilled water for 4 days. The cement pastes were then subjected to a temperature drop from +5 °C to −70 °C at a rate of −0.5 °C/min.

3.3. Tests on mortars

To study the influence of MSWI fly ash on the short-term and middle-term properties of mortars, certain performance characteristics of mortars containing increasing levels of MSWI fly ash were studied. The compositions of the mortars all derive from the composition of standardized mortar as specified in the NF EN 196-1 standard [5]. The fly ash was incorporated in the mortars in place of a fraction of the sand, with all the other components remaining unchanged in relation to the reference mortar. Only cement C1 has been used for this part of the study. Table 2 shows the compositions of the five mortars used.

To study the influence of the soluble fraction of MSWI fly ash, 65 g of ash was washed in 325 g of water for 3 min. Three compositions were studied: mortar M10 (identical to that shown in Table 2), mortar M′10 in which MSWI fly ash was replaced by washed ash and mortar M′0 in which the mixing mortar water was replaced by an ash wash solution.

Table 2
Compositions of the mortars used (in grams)

Mortar	Cement (g)	Water (g)	Ash (g)	Sand (g)	W/C ratio
M0	450	225	0	1350	0.5
M5	450	225	22.5	1327.5	0.5
M10	450	225	45	1305	0.5
M15	450	225	67.5	1282.5	0.5
M20	450	225	90	1260	0.5

The mortar blending times and rates complied with the NF P15-403 standard [7] in all the tests carried out. Blending times specified in this standard are in fact longer than those specified in the NF EN 196-1 standard [5], and were a factor in limiting the segregation observed during preliminary tests carried out with a shorter mixing time.

The flow times recorded using the "LCPC mortar workability meter" were analyzed in accordance with NF P18-452 standard [8] for each composition. The initial and final setting times of the M0, M5, M10, M15 and M20 mortars were measured with the Vicat needle in accordance with the NF P 18-356 standard [9]. Test pieces, $40 \times 40 \times 160$ mm, were placed on the impact test bench in accordance with NF EN 196-1 standard [5] to determine the mechanical strength of M0, M5, M10, M15 and M20 mortars. After setting-up, the mortars were stored in sealed bags until removed from the mold (approximately 3 days). After removal, the test pieces were once again placed in sealed bags and kept at a temperature of 20 °C until the tests were carried out. The ultimate three-point bending tensile strength and compressive strength were determined in accordance with NF EN 196-1 standard [5] after (7, 28, 90, and 565) days. The compressive strengths of the M10 (10% ash), M′10 (10% washed ash) and M′0 (0% ash and washwater) mortars after 28 days were also determined. In this case, the test pieces were kept at 20 °C and 50% relative humidity.

Mass and size variations of the M0, M10 and M20 mortars were also determined after (3, 7, 14, 21, 28 and 35) days. These tests were carried out on test pieces of $20 \times 40 \times 160$ mm for testing size variations, and $40 \times 40 \times 160$ mm for mass variations. The test pieces were kept throughout the duration of the tests at 20 °C and 50% relative humidity.

4. Results and discussion

4.1. Characterization of MSWI fly ash

Fig. 1 shows the size grading curve for the MSWI fly ash. The size grading curves of cement Class C1 (determined by laser granulometry) and sand used in mortar manufacture (determined by sieving) are also shown in comparison. One can observe that the size grading curve of the MSWI fly ash lies between the cement and sand curves and has a larger spread than the other two materials, between 1 and 600 μm approximately.

Table 3 shows the results of the chemical analysis carried out on the MSWI fly ash. The main oxide components of fly ash are (in order of amount): SiO_2, CaO and Al_2O_3. The loss on ignition at 975 °C is also very high (13%). In addition, the ash has high chlorine, sodium and potassium contents. The most abundant heavy metals are zinc and lead. The total

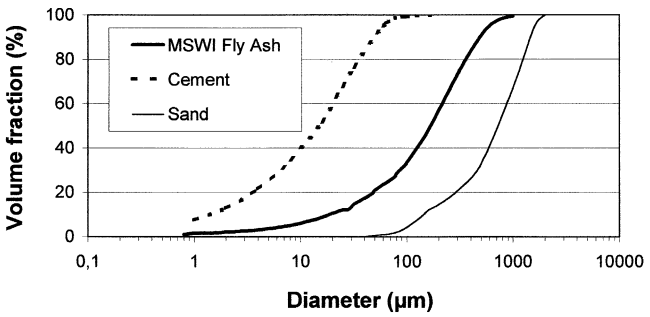

Fig. 1. Size grading curves of cement, MSWI fly ash and sand.

quantity of heavy metal represents approximately 2% of the total mass of the ash. The chemical composition of the ash used is similar to compositions given in the literature [10].

Table 4 shows the main crystalline compounds identified by XRD in the MSWI fly ash. The respective quantities of the different compounds were estimated from the height of the corresponding peaks on the XRD diagrams. The symbol "X" in the column "Quantity" indicates the relative height of the peaks. The most abundant compounds are, in order of size: quartz, sylvite and halite, anhydrite, calcite and lime. These results confirm those obtained by other researchers using similar materials [11,12].

Figs. 2 and 3, respectively, show backscattered electron images of the MSWI fly ash for the two fields of observation, FA1 and FA2. One can see that the MSWI fly ash has various forms, unlike coal fly ash that is composed of spherical particles. Some MSWI fly ash particles are spherical (full or hollow) and a relatively large fraction of the ash appears to have a vitreous form. One can also observe elongated, angular, very porous particles and clusters of sintered particles.

For observation fields FA1 and FA2, X-ray images have also been collected for the following elements: Ca, Si, Al, Fe, Na, K, Cl and S. For each element, the intensity of the response obtained was compared with a threshold intensity (different for each element analysed) above which the element is considered to be present. Superimposing the images collected for the eight elements analysed then allowed us to reconstruct the chemical nature of the different phases of the ash (for more details concerning these imaging techniques, see Refs. [3,13]).

The different phases determined are:[2] S (quartz), AS (aluminosilicate), CAS_2 (calcium aluminodisilicate), $CaCl_2$ (calcium chloride) and $CaSO_4$ (anhydrite). All remaining, nonidentified phases were grouped in a phase called the "inert" phase. Table 5 shows the area fractions for each phase determined for the two fields of observation.

X-ray spectrometric analysis has enabled us to determine the composition of certain phases of the MSWI fly ash. However, this experimental technique, which is regularly used to study the composition of cements, is more difficult to apply to the MSWI ash. Indeed, fly ashes are very heterogeneous and their size grading has a larger spread than cement. Moreover, unlike the main components of cement whose chemical compositions are known, the mineralogical composition of ash is not well known. The analysis of a field of observation of the MSWI ash is not necessarily representative of all ashes given the size of the particles and their heterogeneity. This is why the area fractions of the $CaSO_4$ and S phases determined for the two observations FA1 and FA2 present significant differences (Table 5). A larger number of observations would be necessary to reduce this deviation by averaging. However, since the aim of our research is not a complete and precise mineralogical characterization of the MSWI fly ash, we will assume that the quantitative composition determined here is a sufficient approximation for modelling purposes.

Eight elements in the MSWI ash were analysed by X-ray spectrometry: Ca, Al, Si, Na, K, Fe, Cl and S. These elements represent (as oxides) approximately 80% of the total mass of ash. However, the elements Fe, Na and K were not taken into account in the later hydration modelling for reasons of simplification (for Fe) and because they did not enable us to categorically identify the mineral phases containing them (for Na and K). In addition, a number of minor elements were not analyzed.

Two additional phases were identified by SEM analysis in relation to XRD: aluminosilicate (AS) and calcium aluminodisilicate (CAS_2). The X-ray analysis showed that the MSWI ash particles of these phases contain large proportions of silica and aluminium (and calcium for the CAS_2 phase), but it does not allow us to determine the stoichiometrical coefficients of these elements. In the CaO, Al_2O_3, SiO_2 system, three defined combinations are known: CAS_2, C_2AS and C_3AS [14]. Given the quantity of lime present in MSWI fly ash, the CAS_2 phase appears to be the most probable phase. However, other elements that have not been analyzed could also be a part of the mineralogical composition of these phases.

XRD analysis revealed the presence of halite (NaCl) and sylvite (KCl) in the MSWI fly ash. On the other hand, with X-ray analysis, the response obtained for chlorine corresponds only to that obtained for calcium. The response recorded for the alkalis does not correspond at all to those obtained with chlorine. On the basis of these observations, it would seem that chlorides are present in the form of calcium chloride ($CaCl_2$). However, the detection of alkalies (especially sodium) by X-ray imaging can be difficult. The presence of halite and sylvite in the MSWI ash is mentioned frequently in the literature. The presence of $CaCl_2$ has also been reported [15], but in a less systematic way. We think that chlorides are certainly present in the MSWI ash tested here, mainly in the form of halite and sylvite. Their presence in the form of $CaCl_2$ in small quantities is possible. It is a fact that below a mass percentage of 5%, components are difficult to detect with XRD.

[2] Conventional cement chemistry notation is being used for the fly ash phases, namely C = CaO, S = SiO_2 and A = Al_2O_3.

Table 3
Chemical composition of the MSWI fly ash (LOI, loss on ignition)

Compound	Mass fraction (%)	Compound	Mass fraction (%)	Heavy metals	Content (mg/kg)	Heavy metals	Content (mg/kg)
LOI (975 °C)	13.00	TiO_2	0.84	Zn	11,000	Ni	50
SiO_2	27.23	P_2O_5	0.34	Pb	4000	Se	50
CaO	16.42	Mn_2O_3	0.05	Cu	670	Te	46
AL_2O_3	11.72	SrO	0.01	Mn	600	V	32
Na_2O	5.86	Ba	0.22	Cr	450	Mo	25
K_2O	5.80	Cl	7.20	Cd	270	As	21
MgO	2.52	SO_3	3.00	Sn	180	Co	21
Fe_2O_3	1.80			Sb	110	Tl	<5

4.2. Study of hydration products

Table 6 shows the principal hydrates determined by the XRD tests on the cement pastes without MSWI fly ash (P0–C1 and P0–C2) and with 20% MSWI ash (P20–C1 and P20–C2). The principle crystalline hydrates formed due to the addition of the MSWI ash are ettringite, Friedel's salt and thenardite. These results (in particular formation of ettringite and Friedel's salt) confirm a number of results obtained in other studies [12,15]. The addition of the ash into the cement pastes results also in an increase in quartz and calcite (already present in the ash). The results obtained for the two cements C1 and C2 are very close, except for a significant swelling observed when paste P20–C2 has been removed from the mold (certainly due to the important formation of ettringite).

Fig. 4 shows the results of the DSC tests obtained for cement paste P–C1 and for the cement paste containing 20% MSWI fly ash (in place of cement) P–FA after 28 days (both without immersion).

Fig. 5 shows the DSC curves obtained for pastes P–C1 and P–FA after successive immersion in ethanol, ethylene glycol and distilled water. We can see that the DSC curves of these two cement pastes (after immersion) are very similar.

The DSC tests carried out in the early stages (in particular after 1 and 3 days) have shown that the MSWI ash has a strong influence on cement hydration. After 28 days of hydration, the main feature observed is a movement of the peak corresponding to C–S–H towards negative temperatures for the P–FA paste. As already stated above, the successive immersion of the cement pastes in ethanol, ethylene glycol and distilled water was carried out to replace the interstitial solution of the cement pastes by distilled water and to attempt to determine in this way the origin of the shift of the C–S–H peak (size of the material's pores or concentration of the interstitial solution). After the successive immersion, the two cement pastes both had interstitial solutions of a similar chemical composition (assuming that hydrate dissolution is sufficiently slow). The DSC curves for these cement pastes are practically identical. In particular, the temperature of the C–S–H peak is identical. We can therefore deduce from this result that the porous structures of the C–S–H in the two cement pastes (with or without the MSWI ash) are very similar. The differences observed between the DSC curves of the P–C1 and P–FA pastes after 28 days of hydration must therefore be due essentially to a difference in the chemical composition of the interstitial solutions. A high concentration of soluble alkali in the interstitial solution of the P–FA paste could explain this result.

Table 4
Main compounds in the MSWI fly ash detected by XRD

Compound	Formula	Quantity
Quartz	SiO_2	XXXXX
Calcite	$CaCO_3$	X
Sylvite	KCl	XXX
Halite	NaCl	XXX
Lime	CaO	X
Anhydrite	$CaSO_4$	XX

4.3. Performance characteristics for mortars containing MSWI ashes

Fig. 6 shows the flow times of mortars M0, M5, M10, M15 and M20 measured with the "LCPC mortar workability meter." For the reference mortar M0, three tests were carried out to assess the dispersion of the measurements.

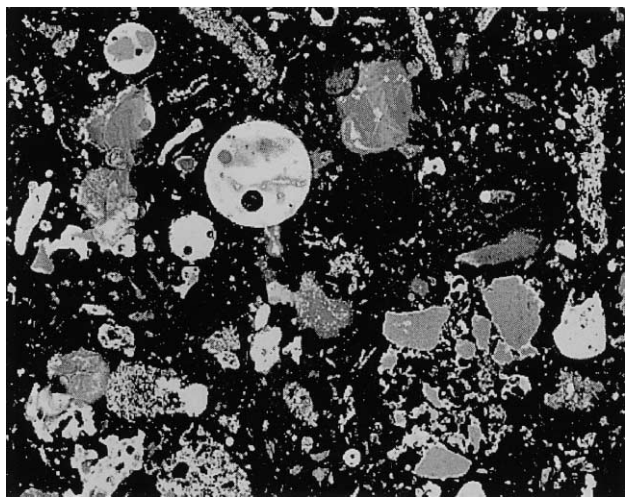

Fig. 2. Observation (FA1) of MSWI fly ash with backscattered electron SEM (approximate size: 500μm×400μm).

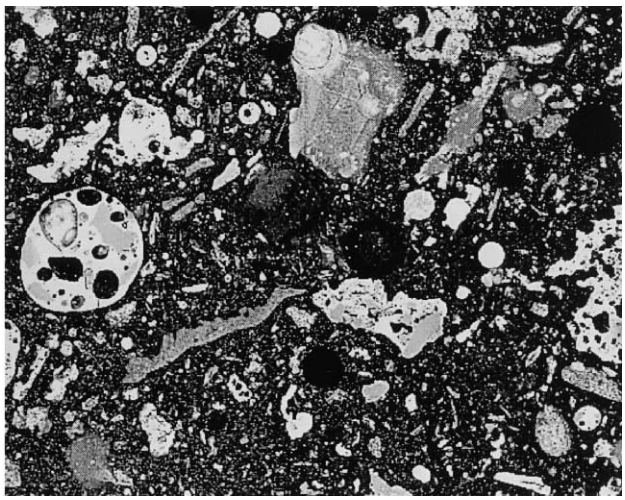

Fig. 3. Observation (FA2) of MSWI fly ash with backscattered electron SEM (approximate size: 500 μm×400 μm).

The standard deviation for these measures was 0.75 s. Given the low value of the standard deviation, one single measurement was performed for the other mortars. We can see that the flow time recorded increases as the ash content increases. It is, however, noteworthy that no problems were encountered with placing the mortars in molds during the preparation of the test specimens.

Fig. 7 shows the initial and final setting times for the M0 to M20 mortars. Incorporating ash in the mortars considerably increases the initial and final setting times. This increase is dramatic when the ash content increases from 10% to 15%. The MSWI fly ash components responsible for delayed setting were not accurately identified. However, a number of studies have already shown that zinc and lead are setting retarders, or may even inhibit setting [16]. These two components are the most abundant heavy metals found in the MSWI ash used.

Fig. 8 shows compressive strengths for the M0, M5, M10, M15 and M20 mortars after (7, 28, 90 and 565) days. In the figure, the error bars represent ±1 S.D. Compressive strengths after 28 days of the M10, M′10 and M′0 mortars are shown in Table 7. From Fig. 8, it would seem that, in general, the mortar compressive strength is optimized for an MSWI ash content of approximately 10% (a lower strength was observed after 28 days, but similar tests carried out with other MSWI ashes did not exhibit this particular feature [17]). Strength increases as ash content is increased to 10%, and falls thereafter. After 90 days, the M10 mortar strength is approximately 15% higher than the M0 control mortar.

Table 5
Area fractions (in %) of the six mineral phases in the MSWI fly ash determined using X-ray spectrometry and SEM analysis

	S	AS	CAS_2	$CaCl_2$	$CaSO_4$	Inert
FA1	13	9	49	18	1.5	9.5
FA2	2.1	12.1	47.4	23.9	6.4	8.1
Average	7.5	10.5	48.2	21	4	8.8

Table 6
Principal hydrates identified in the hydrated cement pastes

Compound	Formula	P0–C1	P0–C2	P20–C1	P20–C2
Quartz	SiO_2	ND	ND	X	X
Calcite	$CaCO_3$	?	?	XX	XX
Portlandite	$Ca(OH)_2$	XXXXX	XXXXX	XXXX	XXXX
Monosulfo-aluminate	$C_3A{\cdot}CS{\cdot}H_{12}$	?	?	ND	ND
Ettringite	$C_3A{\cdot}3CS{\cdot}H_{32}$	X	X	X	XX
Friedel's salt	$C_3A{\cdot}CaCl_2{\cdot}H_{10}$	ND	ND	X	XX
Thenardite	Na_2SO_4	ND	ND	XX	XX

ND, nondetectable. ?, Presence unsure.

On the other hand, the strength of the M20 mortar is approximately 5% lower. The strength of mortars containing MSWI ash increases with time up to 90 days, but the increases in strength due to the presence of ash are obtained generally at a much earlier stage (after 7 days). Strengths obtained after 565 days are lower (M5 mortar presents a decrease in strength of about 10%). However, it is noteworthy that no visible signs of an increase in cracking were observed in these mortars between 90 and 565 days.

Table 7 shows that incorporating washed ash (in M′10 mortar) in place of total ash (M10 mortar) results in a decrease in strength of approximately 20%. On the other hand, however, the incorporation of ash wash water (M′0 mortar) results in an increase in strength of 35% in relation to the M10 mortar.

Incorporating MSWI fly ash in mortars (below 15% with an optimum for 10% ash) provides increased mechanical strength in the medium term (between 28 and 90 days). Several assumptions may be put forward to explain these results.

Firstly, the increase in strength after 7 days due to the presence of ash is most likely not attributable to the potential pozzolanic properties of this waste material. Indeed, pozzolanic reactions are slow and their influence is only evident after longer periods (usually between 28 and 90 days). In the cases observed, gains in strength is important after 7 days and the presence of the ash causes a decrease in mortar strength in the long term (565 days).

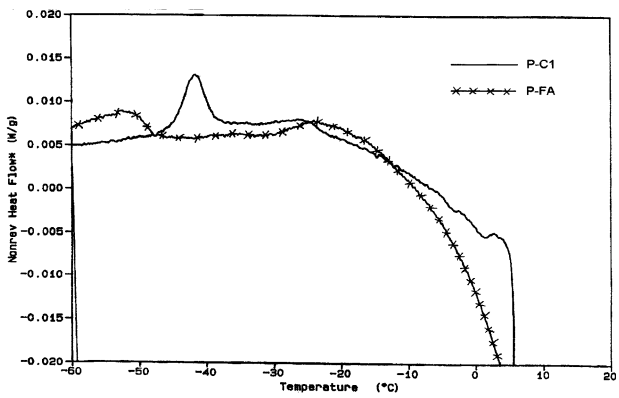

Fig. 4. DSC curves obtained for the cement pastes P–C1 and P–FA after 28 days without immersion.

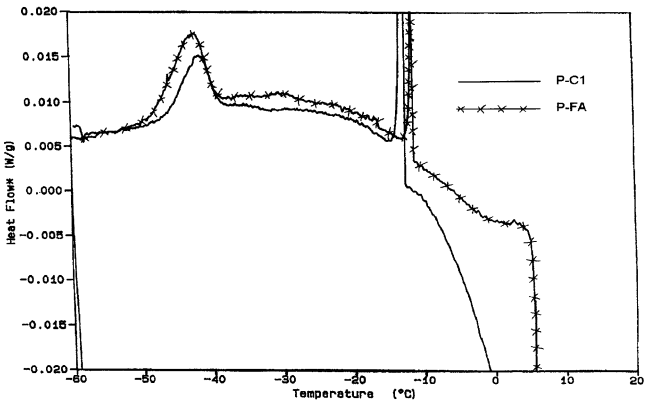

Fig. 5. DSC curves obtained for the P–C1 and P–FA pastes after successive immersions.

The pozzolanic activity of the MSWI fly ash is not necessarily zero, but is in any case very low and does not account for observable increases in strength.

The tests carried out with wash water (M′0 mortar) show that the soluble fraction of the ash allows a considerable increase in compressive strength. The presence of considerable quantities of chlorides in the ash wash water is certainly the cause of this increase in strength. Indeed, chlorides are well-known setting accelerators [16].

The nonsoluble (or low-soluble) fraction of the ash seems conversely to have a negative effect on compressive strength. Indeed, the compressive strength of the M10 mortar is lower than that of the M′0 mortar (made using ash wash water). The quantity of chlorides contained in the two mortars is nevertheless very close. Indeed, analysis of the solution extracted during washing shows that the chlorides were almost completely extracted during this washing process [18]. Elsewhere, the compressive strength of mortar containing 10% washed ash is lower than that of the M10 mortar. Our research has not been conclusive in explaining categorically the influence of the nonsoluble fraction of ash on reductions in compressive strength. One of the explanations we can nevertheless suggest is the following: the MSWI ash particles

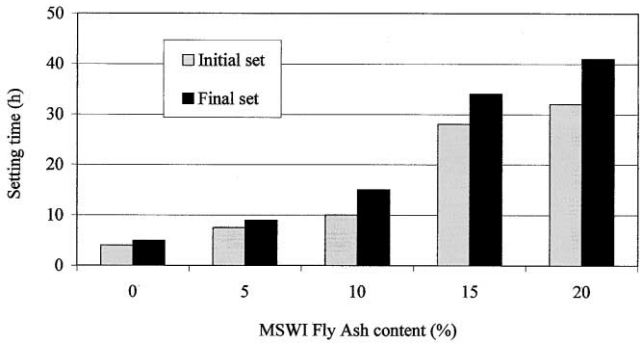

Fig. 7. Initial and final setting times for the M0, M5, M10, M15 and M20 mortars.

could be weak points in mortars. Kessler et al. [15] have shown, based on a SEM analysis of cement pastes containing MSWI fly ash, that the cement paste/fly ash bond appears to be relatively weak.

Competition between the positive effect of chlorides and the negative effect of the nonsoluble fraction could explain the optimal strength obtained for an ash content equivalent to 10%. For ash contents of over 10%, the negative effect of the nonsoluble fraction could become predominant and cause the observed decrease in mechanical strength.

Given the reduced workability of mortars incorporating the MSWI fly ash, one could also impute the increase in strength to absorption of water by the ashes during mixing. We have shown [18] that the higher the ash content, the higher the water demand of mortars containing these MSWI ashes. According to these tests, the MSWI fly ash "absorbs" approximately 28% of its mass in water. This water absorption then diminishes the effective W/C ratio of the cement paste, thus increasing its strength. The effective W/C ratio of the cement paste in M10 mortar (respectively, M20) would in this case be 0.47 (respectively, 0.44). However, although this mechanism certainly tends towards increasing strength, it does not counteract the unfavourable effect of the nonsoluble fraction of the ash. Finally, the decrease in strength observed after 565 days for mortars containing MSWI

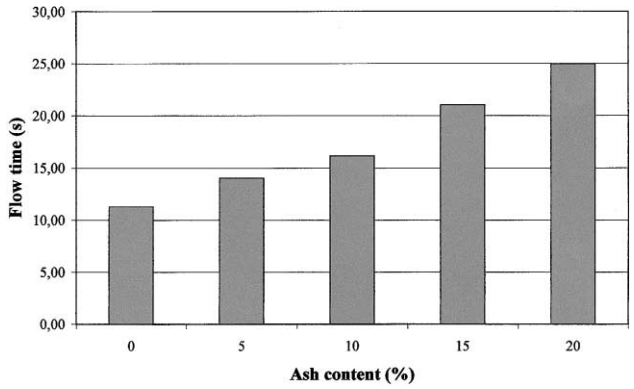

Fig. 6. Flow times of the M0, M5, M10, M15 and M20 mortars.

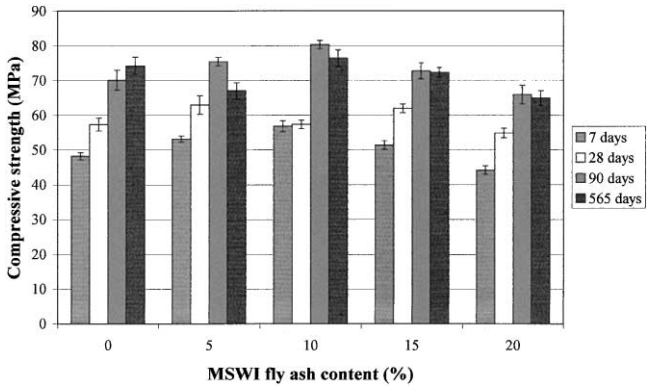

Fig. 8. Compressive strengths of the M0, M5, M10, M15 and M20 mortars after 7, 28, 90 and 565 days.

Table 7
Compressive strengths after 28 days of the M10, M′10 and M′0 mortars kept at 20 °C and 50% relative humidity

	Compressive strength (MPa)
M10	51.3
M′10	40.6
M′0	69.0

fly ash could not be explained. Certain MSWI ash components are aggressive species for cement (sulphates and alkalis in particular) and may provoke degradation of the mortars. However, it is surprising that this decrease in strength should occur in the long term (after 565 days), under conditions of nonaggressive storage (20 °C, in sealed bags).

Figs. 9 and 10 present, respectively, the size and the mass variations of mortars M0, M10 and M20 determined over a period of approximately 5 weeks after removing the molds. One can see in Fig. 9 that the shrinkages of the two mortars containing ash (M10 and M20) are practically identical. Up to 7 days, shrinkage of the two mortars containing ash is approximately twice that of the control mortar M0. Beyond that, their respective evolution is comparable. In Fig. 10, one can see that mass variations of M10 and M20 mortars are lower than those of the control mortar M0.

In consideration of the small size of the test pieces used, thermal shrinkage of the mortars may be ignored. The shrinkage measured is thus due, on one hand, to the evacuation of water from the test pieces and, on the other, to the autogenous shrinkage caused by Le Chatelier's contraction principle. The lower shrinkage values of M0 mortar cannot be explained by drying shrinkage. Indeed, mortars containing ash lose less water than the M0 mortar (Fig. 10). The increase in shrinkage of these two mortars would therefore seem to be due to an increase in autogenous shrinkage.

The lower water loss of these mortars in relation to the M0 mortar can be explained by the immobilization of water due to hydration product formation. Thus, the high chloride and sulphate content of the MSWI fly ash may result in the formation of high quantities of ettringite and chloroaluminates (hydrates which mobilise a large number of water molecules). The early formation of these two hydrates could explain the high shrinkage of mortars containing fly ash observed in early stages.

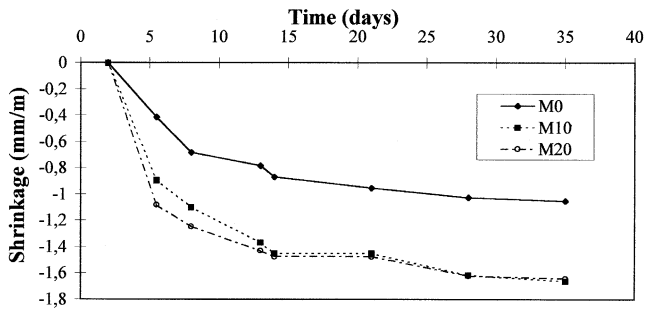

Fig. 9. Size variations of the M0, M10, and M20 mortars.

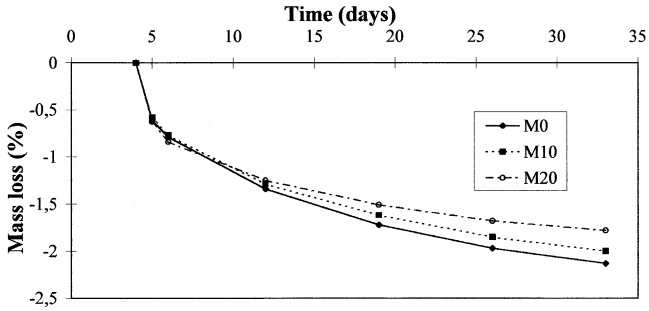

Fig. 10. Mass variation of the M0, M10 and M20 mortars.

5. Conclusion

The physico-chemical and mineralogical characteristics of a MSWI fly ash have been studied. This fly ash has a coarser and wider size grading than that of typical cements. It contains a high soluble fraction made up mainly of chlorides and sulphates. The sulphates are principally present in the form of anhydrite. Chlorides are certainly present in the form of halite and sylvite, though the presence of calcium chloride is also a possibility. Two phases possibly possessing pozzolanic properties have also been identified: a calcium aluminodisilicate (CAS_2) and an aluminosilicate (AS). This fly ash also contains high quantities of heavy metals (approximately 2%), of which the most abundant are zinc and lead. This research has allowed us to propose a simplified quantitative mineralogical composition for this fly ash.

We have also studied hydration products formed in cement pastes in the presence of the MSWI fly ash. Analysis by XRD has demonstrated the presence of Friedel's salt, ettringite and thenardite resulting from the presence of fly ash. DSC analyses have shown that cement pastes containing MSWI fly ash have a more concentrated interstitial solution than pure cement pastes. Tests carried out on samples in which the pore solution was replaced have allowed us to conclude that the C–S–H structure in cement pastes containing fly ash is very close to that of pure cement pastes.

The performance characteristics of mortars with increasing MSWI fly ash content (up to 20% of the cement mass) have been determined. This study has shown that the MSWI fly ash increases mortar setting times. The retarding effect of zinc and lead is almost certainly the cause of the delayed setting times. Incorporating MSWI fly ash in mortars, up to 15% (with an optimum for 10%) in relation to the cement mass, increases their strength after (7, 28, and 90) days. The acceleration effect of chloride almost certainly explains this

increase. Beyond 15%, the fly ash causes a slight decrease in strength, which may be due partly to the weak bond between the cement paste and the MSWI fly ash. Strength reductions in the longer term (after 565 days) were observed in all the mortars containing MSWI fly ash. This decrease in strength, occurring under nonaggressive storage conditions, has not been explained.

This experimental study has allowed us to propose an approximate quantitative mineralogical composition for the MSWI fly ash to incorporate it into the CEMHYD3D cement hydration model and to take into consideration its interactions with cement components. Assumptions of the model and the results obtained using it will be presented in the second part of this article.

Acknowledgments

One of the authors, S. Rémond, would like to thank ADEME for their financial support. The authors also thank Vicat, which carried out the chemical and size grading analyses of the MSWI fly ash, and Cylergie, for interpreting the fly ash and cement paste XRD diagrams. The assistance of Paul Stutzman (BFRL/NIST) in performing the SEM analysis is greatly appreciated. S. Rémond would also like to thank the staff of BFRL for their hospitality during his 6-month stay at NIST.

References

[1] S. Rémond, Evolution de la microstructure des bétons contenant des déchets au cours de la lixiviation, PhD Thesis, Ecole Normale Supérieure de Cachan, defended November 17, 1998.
[2] S. Rémond, P. Pimienta, P. Kalifa, Incorporating waste into the preparation of concrete: bases for an assessment methodology, Second International Conference Building and the Environment, Paris, 9–12 juin 1997, CSTB, Paris, 1997, pp. 659–668.
[3] D.P. Bentz, Three-dimensional computer simulation of Portland cement hydration and microstructure development, J. Am. Ceram. Soc. 80 (1997) 3–21.
[4] D.P. Bentz, E.J. Garboczi, A digitized simulation model for microstructural development, Adv. Cem. Mater., Ceram. Trans. 16 (1991) 211–226.
[5] NF EN 196-1, août 1995, Méthodes d'essais des ciments—Détermination des résistances mécaniques.
[6] D.P. Bentz, P.E. Stutzman, SEM analysis and computer modelling of hydration of Portland cement particles, in: S.M. DeHayes, D. Stark (Eds.), Petrography of Cementitious Materials, ASTM, Philadelphia, PA, 1994, p. 60.
[7] NF P 15-403, juillet 1963, Liants hydrauliques—Techniques des essais, sable et mortier normal.
[8] NF P 18-452, mai 1988, Bétons—Mesure du temps d'écoulement des bétons et des mortiers aux maniabilimètres.
[9] NF P 18-356, août 1985, Adjuvants pour bétons, mortiers et coulis—Détermination du temps de prise sur mortiers.
[10] A. Bouchelaghem, Solidification/stabilisation des DIS, Rev. Tech. APAVE 262 (1993).
[11] G. Escadeillas, S. Julien, A. Vaquier, Amélioration des matériaux de construction non armés utilisant des cendres d'incinération d'ordures ménagères, Congrès International sur les Procédés de Solidification et de Stabilisation des déchets, Nancy, France, 1995.
[12] R. Derie, Réactivité des cendres volantes d'incinérateurs de déchets ménagers: Expérience de percolation en laboratoire, Trib. Eau 564 (4) (1993) 11–18.
[13] D.P. Bentz, P.E. Stutzman, C.J. Haecker, S. Remond, SEM/X-ray imaging of cement-based materials, in: H.S. Pietersen, J.A. Larbi, H.H.A. Janssen (Eds.), Proceedings of the 7th Euroseminar on Microscopy Applied to Building Materials, Delft University of Technology, 1999, pp. 457–466.
[14] M. Duriez, J. Arrambide, Nouveau Traité de Matériaux de Construction, Part I, second ed., Dunod, Paris, 1961.
[15] B. Kessler, M. Rollet, F. Sorrentino, Microstructure of cement pastes as incinerator ash host, in: R.W. Piggot (Ed.), Proceedings of the First International Symposium on Cement Industry Solution to Waste Management, Calgary, 1992, pp. 235–251.
[16] H.F.W. Taylor, Cement Chemistry, Thomas Telford, London, 1997.
[17] S. Rémond, Incorporation de cendres volantes d'usines d'incinération dans les mortiers, Mémoire de DEA, DEA MAISE, ENS de Cachan, June 30, 1995.
[18] S. Rémond, P. Pimienta, N. Rodrigues, J.P. Bournazel, Assessing the properties of mortars containing Municipal Solid Waste Incineration fly ash, International Congress, Creating with Concrete, University of Dundee, September 6–10, 1999, (1999) 319–326.